



Cite this: *Chem. Commun.*, 2016, 52, 10992

Received 24th July 2016,
Accepted 5th August 2016

DOI: 10.1039/c6cc06102h

www.rsc.org/chemcomm

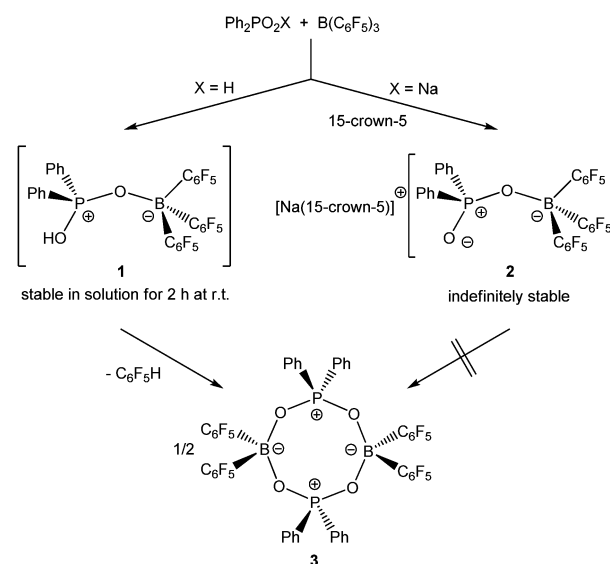
Increasing the Brønsted acidity of $\text{Ph}_2\text{PO}_2\text{H}$ by the Lewis acid $\text{B}(\text{C}_6\text{F}_5)_3$. Formation of an eight-membered boraphosphinate ring $[\text{Ph}_2\text{POB}(\text{C}_6\text{F}_5)_2\text{O}]_2$ †

Ralf Kather,^a Elena Rychagova,^b Paula Sanz Camacho,^c Sharon E. Ashbrook,^c J. Derek Woollins,^c Lars Robben,^a Enno Lork,^a Sergey Ketkov^{*b,d} and Jens Beckmann^{*a}

Autoprotolysis of the metastable acid $(\text{C}_6\text{F}_5)_3\text{BOPPh}_2\text{OH}$, prepared *in situ* by the reaction of the rather weak Brønsted acid $\text{Ph}_2\text{PO}_2\text{H}$ with the strong Lewis acid $\text{B}(\text{C}_6\text{F}_5)_3$, gave rise to the formation of the eight-membered ring $[\text{Ph}_2\text{POB}(\text{C}_6\text{F}_5)_2\text{O}]_2$ and $\text{C}_6\text{F}_5\text{H}$. The conjugate base was isolated as stable sodium crown ether salt $[\text{Na}(15\text{-crown-5})][\text{Ph}_2\text{PO}_2\text{B}(\text{C}_6\text{F}_5)_3]$.

Lewis acids can significantly increase the acidity of Brønsted acids.¹ This principle is operative in the prototypical Lewis pair complex $(\text{C}_6\text{F}_5)_3\text{BOH}_2$, the adduct of the electron pair acceptor $\text{B}(\text{C}_6\text{F}_5)_3$ and the electron pair donor H_2O .² In MeCN, the acidity of $(\text{C}_6\text{F}_5)_3\text{BOH}_2$ ($\text{p}K_{\text{a}} = 8.4$) is very similar to that of HCl ($\text{p}K_{\text{a}} = 8.5$).³ Thus, $(\text{C}_6\text{F}_5)_3\text{BOH}_2$ is a strong acid that readily protonates basic organic⁴ and organometallic compounds.^{2,5} Diphenylphosphinic acid, $\text{Ph}_2\text{PO}_2\text{H}$, is a rather weak acid. As it is well-known that $\text{B}(\text{C}_6\text{F}_5)_3$ forms Lewis pair complexes with phosphine oxides,⁶ we were curious to study if $\text{B}(\text{C}_6\text{F}_5)_3$ will also increase the Brønsted acidity of $\text{Ph}_2\text{PO}_2\text{H}$.

Upon dissolving $\text{Ph}_2\text{PO}_2\text{H}$ and $\text{B}(\text{C}_6\text{F}_5)_3$ in CDCl_3 , multinuclear NMR spectroscopy indeed indicates the formation of a single product that was assigned to $(\text{C}_6\text{F}_5)_3\text{BOPPh}_2\text{OH}$ (**1**) (Scheme 1). The ^{31}P NMR spectrum (CDCl_3) of **1** shows signal at $\delta = 42.1$ ppm that differs substantially from that of $\text{Ph}_2\text{PO}_2\text{H}$ (33.9 ppm). The ^{11}B NMR spectrum (CDCl_3) of **1** exhibits a broad signal at $\delta = -1.3$ ppm, which is significantly different



Scheme 1 Formation and reactivity of **1** and its stable sodium salt **2**.

from that of $\text{B}(\text{C}_6\text{F}_5)_3$ (59.0 ppm). Solutions in CDCl_3 show a limited stability and all attempts to isolate **1** by removal of the solvents failed. However, these solutions are stable at r.t. for 2 h; within this time NMR spectroscopy gave no evidence for the formation of other species. While the acid **1** could not be isolated, the reaction of $\text{Ph}_2\text{PO}_2\text{Na}$, $\text{B}(\text{C}_6\text{F}_5)_3$ and 15-crown-5 provided the indefinitely stable, conjugate base $[\text{Na}(15\text{-crown-5})][\text{Ph}_2\text{PO}_2\text{B}(\text{C}_6\text{F}_5)_3]$ (**2**), which was obtained as colourless crystals in 73% yield (Scheme 1). The ^{31}P and ^{11}B NMR spectra ($\text{THF}-d_6$) gave signals at $\delta = 22.3$ and -2.7 ppm. The molecular structure of **2** reveals that the $[\text{Na}(15\text{-crown-5})]^+$ ion and the $[\text{Ph}_2\text{PO}_2\text{B}(\text{C}_6\text{F}_5)_3]^-$ ion are associated by a $\text{Na} \cdots \text{O}$ contact (Fig. 1). When a solution of **1** in CDCl_3 was kept standing for a few hours or heated under reflux for a few minutes NMR spectroscopy indicates the formation of new species, which were identified as the eight-membered boraphosphinate ring $[\text{Ph}_2\text{POB}(\text{C}_6\text{F}_5)_2\text{O}]_2$ (**3**) and

^a Institut of Inorganic Chemistry and Crystallography, Bremen University, Leobener Straße, 28359 Bremen, Germany. E-mail: j.beckmann@uni-bremen.de

^b G. A. Razuvaev Institute of Organometallic Chemistry RAS, 49 Tropinin St., 603950 Nizhny Novgorod, Russian Federation. E-mail: sketkov@iomc.ras.ru

^c EaStChem. School of Chemistry, University of St. Andrews, St. Andrews, Fife KY16 9ST, UK

^d N. I. Lobachevsky Nizhny Novgorod State University, Gagarin ave. 23, 603950 Nizhny Novgorod, Russian Federation

† Electronic supplementary information (ESI) available: Experimental section, NMR spectra, X-ray crystallography, X-ray powder diffraction, computational details, additional references. CCDC 1480495 and 1411098–1411113. For ESI and crystallographic data in CIF or other electronic format see DOI: 10.1039/c6cc06102h



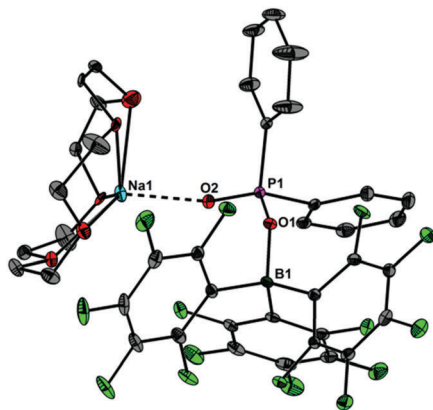


Fig. 1 Molecular structure of **2** showing 30% probability ellipsoids and the crystallographic numbering scheme. Selected bond parameters [\AA , $^\circ$]: B1–O1 1.508(2), P1–O1 1.544(1), P1–O2 1.482(1), Na1–O2 2.211(2), B1–O1–P1 134.5(1).

$\text{C}_6\text{F}_5\text{H}$. On a preparative scale, **3** was isolated in 76% yield when a solution of **1** prepared *in situ* from $\text{Ph}_2\text{PO}_2\text{H}$ and $\text{B}(\text{C}_6\text{F}_5)_3$, in toluene was heated overnight under reflux (Scheme 1). This reactivity resembles the autoprotolysis of $(\text{C}_6\text{F}_5)_3\text{BOH}_2$ at elevated temperatures giving rise to the formation of $[(\text{C}_6\text{F}_5)_2\text{BOH}]_3$ and $\text{C}_6\text{F}_5\text{H}$.⁷ The eight-membered boraphosphinate ring **3** seems to be the first member of this compound class, however, we note the closely related series of cubic boraphosphonate cages in the literature comprising similar eight-membered ring subunits within the cage structure.⁸ The ^{31}P and ^{11}B NMR spectra (CDCl_3) of **3** revealed signals at $\delta = 37.8$ and 6.3 ppm, but no coupling information. The molecular structure of **3** comprises a strongly puckered $\text{B}_2\text{P}_2\text{O}_4$ ring (puckering factor = 0.890), whereas isolobal eight-membered siloxane rings are usually almost planar (Fig. 2).⁹ The bond parameters of **3** are very similar to those of the cubic boraphosphonate cages.⁸ In a failed attempt to isolate **1** by crystallisation, a small crop of single crystals **4** was isolated, which turned out to be a hydrogen-bonded complex between

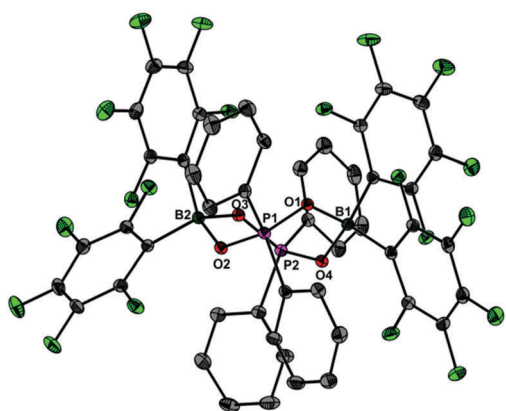
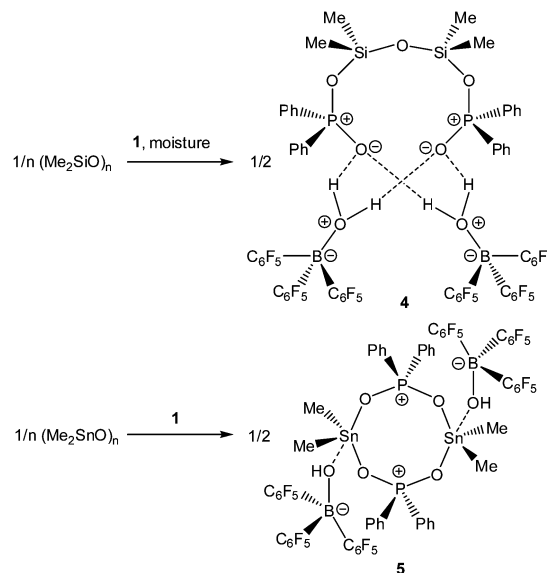


Fig. 2 Molecular structure of **3** showing 30% probability ellipsoids and the crystallographic numbering scheme. Selected bond parameters [\AA , $^\circ$]: B1–O1 1.501(3), B1–O4 1.507(3), B2–O2 1.506(3), B2–O3 1.513(3), P1–O1 1.538(2), P1–O2 1.537(2), P2–O3 1.534(2), P2–O4 1.539(2), B1–O1–P1 129.2(1), B1–O4–P2 129.1(1), B2–O2–P1 128.8(1), B2–O3–P2 134.2(1).



Scheme 2 Reactivity of **1** towards polymeric group 14 oxides $(\text{Me}_2\text{SiO})_n$ and $(\text{Me}_2\text{SnO})_n$.

two molecules of $(\text{C}_6\text{F}_5)_3\text{BOH}_2$ and the disiloxadiphosphate $[\text{Ph}_2\text{P}(\text{O})\text{OSiMe}_2]_2\text{O}$. The formation of **4** can be rationalized by the accidental cleavage of silicon grease used to seal the joints and stopcocks (Scheme 2).¹⁰ The facile cleavage of siloxanes is remarkable and points to the high Brønsted acidity of **1**. Variation of the stoichiometric ratio of the reactants gave no other product than **4**. The O...O donor acceptor distances (2.542(5), 2.684(4), 2.681(4), 2.559(4) \AA) are indicative of medium strength hydrogen bonding.¹¹ The ^{31}P , ^{29}Si and ^{11}B NMR spectra ($\text{THF}-d_8$) of **4** show signals at $\delta = 32.4$, -23.9 and 3.4 ppm. The molecular structure of **4** comprises a novel hydrogen bond motif featuring two BOH_2 hydrogen bond donors and two PO hydrogen acceptors (Fig. 3). The hydrogen bond motif can be described as binary graph set $R_4^4(8)$ ¹² and is strongly reminiscent to that of $(\text{Ph}_3\text{SiOH})_4$,¹³ in which four silanol groups serve as donors and acceptors.

To provide a quantitative description of the Brønsted acidity increase upon going from $\text{Ph}_2\text{PO}_2\text{H}$ to **1** and to reveal the corresponding electronic structure changes we carried out DFT calculations of these acids and the conjugate bases with use of the Gaussian09 package.¹⁴ The optimized molecular geometries agree well with the experimental data for **2** (Fig. 1), $[\text{Ph}_2\text{PO}_2]^-$ and $\text{Ph}_2\text{PO}_2\text{H}$ ¹⁵ (Table S2, see ESI[†]). The difference in the dissociation enthalpies of $\text{Ph}_2\text{PO}_2\text{H}$ and **1** (eqn (1) and (2)) $\Delta\Delta H = \Delta H_1 - \Delta H_2$ is estimated at the M052X/6-31+G** level of theory as 34.0 kcal mol^{-1} (gas phase) and 14.1 kcal mol^{-1} (MeCN solution). These values are indicative of much higher Brønsted acidity of **1** as compared to that of the $\text{Ph}_2\text{PO}_2\text{H}$. Our calculations of atomic charges show that the O–H bond becomes more polar upon going from $\text{Ph}_2\text{PO}_2\text{H}$ to **1** (Table S3, see ESI[†]). Calculated deformation electron densities (DED) reveal a weakening of the O–H covalent bonding upon coordination of $\text{B}(\text{C}_6\text{F}_5)_3$ to $\text{Ph}_2\text{PO}_2\text{H}$ (Fig. S35, see ESI[†]).



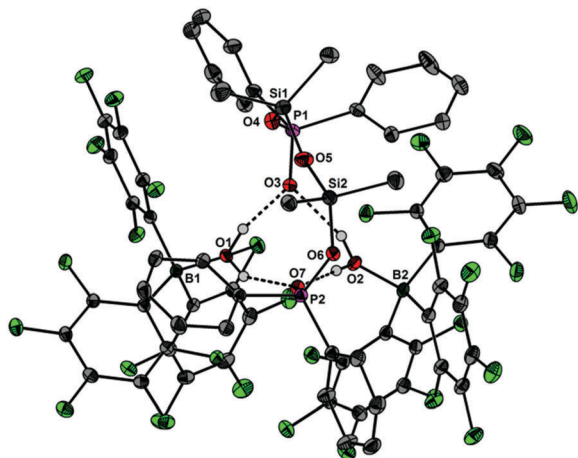
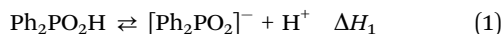


Fig. 3 Molecular structure of **4** showing 30% probability ellipsoids and the crystallographic numbering scheme. Selected bond parameters [Å, °]: B1–O1 1.562(5), B2–O2 1.556(5), P1–O3 1.492(3), P1–O4 1.558(4), P2–O6 1.567(3), P2–O7 1.502(3), Si1–O4 1.650(4), Si1–O5 1.613(4), Si2–O5 1.611(4), Si2–O6 1.668(3), P1–O4–Si1 149.7(2), P2–O6–Si2 143.8(2), Si1–O5–Si2 159.1(3), O1···O3 2.542(5), O1···O7 2.684(4), O2···O3 2.681(4), O2···O7 2.559(4).

These changes in the electronic structures explain the increased Brønsted acidity of **1**. The $\Delta H_1 - \Delta H_2$ enthalpy change is equal to the $\Delta H_3 - \Delta H_4$ difference in the B–O bond dissociation energies in the $[\text{Ph}_2\text{PO}_2\text{B}(\text{C}_6\text{F}_5)_3]^-$ anion and **1** (eqn (3) and (4)).



The B–O bond in $[\text{Ph}_2\text{PO}_2\text{B}(\text{C}_6\text{F}_5)_3]^-$ is expected, therefore, to be stronger than that in **1**. Indeed, the DED maps (Fig. S36, see ESI†) demonstrate a higher B–O deformation density in the anion. This stabilization of $[\text{Ph}_2\text{PO}_2\text{B}(\text{C}_6\text{F}_5)_3]^-$ also contributes to the higher Brønsted acidity of **1**. To compare the acidities of $\text{Ph}_2\text{PO}_2\text{H}$ and **1** with those of other acids we calculated¹⁶ the pK_a values in the gas phase and MeCN solution for a series of 15 compounds with tabulated experimental data in the ranges of $pK_{a(\text{gas})} = 209\text{--}251$ and $pK_{a(\text{MeCN})} = 0\text{--}30$ (Tables S4 and S5, see ESI†). On the basis of the linear regressions between experimental and calculated pK_a values (Fig. S37 and S38, see ESI†) the expected pK_a values for $\text{Ph}_2\text{PO}_2\text{H}$ and **1** were found to be, respectively, 239.2 and 214.4 in the gas phase and 20.5 and 9.4 in MeCN solution. The gas-phase acidity of **1** appears to be stronger than that of $\text{CF}_3\text{SO}_3\text{H}$ ($pK_{a(\text{gas})} 219.6$)¹⁷ while in MeCN solution **1** is comparable with HCl and tosylic acid ($pK_{a(\text{MeCN})} 8.5^3$ and 8.6^{18} respectively).

In light of the remarkable siloxane bond cleavage, we have started to elaborate the reactivity of **1** towards other element oxides. Indeed, the reaction of polymeric $(\text{Me}_2\text{SnO})_n$ with **1** rapidly occurred at r.t. and produced the eight-membered $\text{Sn}_2\text{P}_2\text{O}_4$ heterocycle $[\text{Me}_2\text{Sn}(\text{OPPh}_2\text{O})_2\text{SnMe}_2][\text{HO}(\text{C}_6\text{F}_5)_3]_2$ (**5**) in 83% yield (Scheme 2). The ¹¹⁹Sn and ³¹P MAS NMR spectra

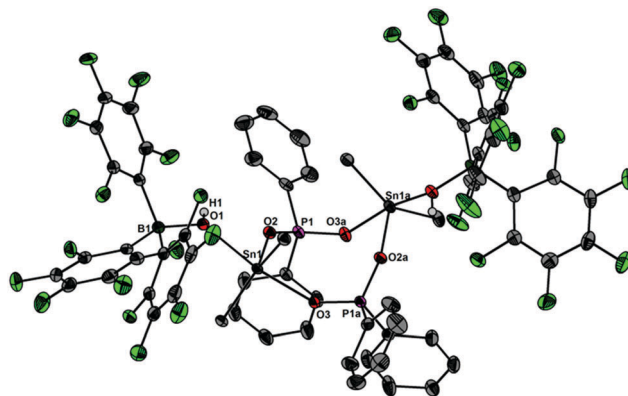
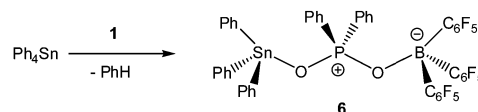


Fig. 4 Molecular structure of **5** showing 30% probability ellipsoids and the crystallographic numbering scheme. Selected bond parameters [Å, °]: B1–O1 1.512(3), P1–O2 1.538(2), P1–O3a 1.515(2), Sn1–O1 2.231(2), Sn1–O2 2.040(2), Sn1–O3a 2.156(2), B1–O1–Sn1 133.5(2), P1–O2–Sn1 139.5(1), P1–O3a–Sn1a 138.1(1).

show broad signals at $\delta = -180.5$ ppm and 31.2 ppm. Freshly prepared solutions of phase-pure **5** (checked by powder diffraction) in CDCl_3 shows four ¹¹⁹Sn NMR signals and three ³¹P NMR signals, which point to a reversible dynamic process that is not yet understood in full detail (see ESI†). Similar solution behaviour was observed for the related heterocycles $[\text{R}_2\text{Sn}(\text{OPPh}_2\text{O})_2\text{SnR}_2][\text{O}_3\text{SCF}_3]_2$ (R = Ph, *t*-Bu), which were obtained by the reaction of $(\text{Ph}_2\text{SnO})_n$ or $(\text{t-Bu}_2\text{SnO})_3$ with $\text{Ph}_2\text{PO}_2\text{H}$ and triflic acid.¹⁹ On a longer time scale (several weeks) **5** shows signs of irreversible decomposition in solution and in the solid-state. In both states, the same unassigned decomposition product with a ¹¹⁹Sn chemical shift of $\delta = 71.1$ ppm slowly forms. The molecular structure of **5** contains a strongly puckerred $\text{Sn}_2\text{P}_2\text{O}_4$ ring (puckering factor = 0.888)⁹ that resembles that of the slightly less puckerred $[\text{t-Bu}_2\text{Sn}(\text{OPPh}_2\text{O})_2\text{Sn}(\text{t-Bu}_2)]_2[\text{O}_3\text{SCF}_3]_2$ (puckering factor = 0.921) (Fig. 4).¹⁹ The spatial arrangement of the Sn atoms is distorted trigonal bipyramidal (geometrical goodness = 89.7°)²⁰ and defined by a C_2O_3 donor set. The Sn–O bond lengths within the ring (2.040(2) and 2.156(2) Å) are shorter than that of the exocyclic $\text{HO}(\text{C}_6\text{F}_5)_3$ moiety (2.231(2) Å). The same trend was observed for $[\text{t-Bu}_2\text{Sn}(\text{OPPh}_2\text{O})_2\text{Sn}(\text{t-Bu}_2)]_2[\text{O}_3\text{SCF}_3]_2$,¹⁹ in which the endocyclic Sn–O bonds (2.045(3) and 2.173(4) Å) are shorter than the Sn–O bond length related with the triflate moiety (2.303(1) Å). It might be speculated that the longer Sn–O bonds are subject to electrolytic dissociation, which could explain the dynamic behaviour in solution. We finally studied the reactivity of **1** towards Ph_4Sn , which proceeded with facile phenyl group cleavage providing $\text{Ph}_3\text{SnOPPh}_2\text{OB}(\text{C}_6\text{F}_5)_3$ in 86% yield (Scheme 3). This reaction closely resembles the quantitative reaction of Ph_4Sn with triflic acid giving rise



Scheme 3 Phenyl group cleavage in Ph_4Sn using **1**.



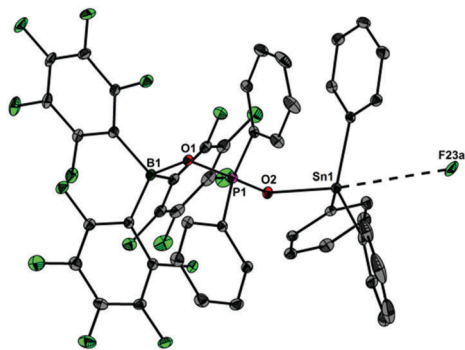


Fig. 5 Molecular structure of **6** showing 30% probability ellipsoids and the crystallographic numbering scheme. Selected bond parameters [Å, °]: B1–O1 1.527(2), P1–O1 1.521(1), P1–O2 1.527(1), Sn1–O2 2.058(1), Sn1–F23a 3.392(3), B1–O1–P1 139.9(1), P1–O2–Sn1 142.29(7).

to the formation $\text{Ph}_3\text{SnO}_3\text{SCF}_3$.²¹ The ^{119}Sn NMR spectrum (CDCl_3) of **6** shows a doublet centred at $\delta = -59.6$ ppm with a $^2J(^{119}\text{Sn}-\text{O}-^{31}\text{P})$ coupling of 146 Hz, which suggests that the Sn atoms are tetracoordinate in solution (Fig. 5). In the solid-state, **6** comprises a 1D coordination polymer with distorted trigonal bipyramidal Sn atoms (geometrical goodness = 51.6°)²⁰ defined by a C_3OF donor set.

The Brønsted acidity of $\text{Ph}_2\text{PO}_2\text{H}$ was significantly increased upon addition of the Lewis acid $\text{B}(\text{C}_6\text{F}_5)_3$ giving rise to $(\text{C}_6\text{F}_5)_3\text{BOPPh}_2\text{OH}$ (**1**) in solution. Unlike its conjugate base $[\text{Na}(15\text{-crown-5})][\text{Ph}_2\text{PO}_2\text{B}(\text{C}_6\text{F}_5)_3]$ (**2**), the acid **1** is thermally unstable and undergoes autoprotolysis and formation of the boraphosphinate ring $[\text{Ph}_2\text{POB}(\text{C}_6\text{F}_5)_2\text{O}]_2$ (**3**) and $\text{C}_6\text{F}_5\text{H}$. Despite its limited life span, **1** can be used for synthetic purposes, as was demonstrated for two examples from organotin chemistry. The stable water adduct $(\text{C}_6\text{F}_5)_3\text{BOH}_2$ is known to bind up to two additional water molecules *via* hydrogen bonding, *e.g.* $(\text{C}_6\text{F}_5)_3\text{BOH}_2 \cdot 2\text{H}_2\text{O}$,²² which adversely affects the stoichiometric control of protonation reactions. Moreover, the various related anions, *e.g.* $[\text{HOB}(\text{C}_6\text{F}_5)_3]^-$, $[\text{HO}\{\text{B}(\text{C}_6\text{F}_5)_3\}_2]^-$ and $[\text{O}\{\text{B}(\text{C}_6\text{F}_5)_3\}_2]^{2-}$,^{2,4} suggest that hydroxide and oxide ions may be also transferred upon protonation. These adverse properties have not been observed for **1**. We are currently investigating if the acidity of other Brønsted acids, such as sulfonic and sulfonic acids, may be also increased by applying the same concept.

The Deutsche Forschungsgemeinschaft (DFG) is gratefully acknowledged for financial support. The theoretical part of this work was supported by the Russian Science Foundation (Project 14-13-00832). We thank Dr Daniel Himmel (Universität Freiburg) for an invaluable discussion about $\text{p}K_a$ value calculations.

Notes and references

- Superacid Chemistry*, ed. G. A. Olah, G. K. S. Prakash, A. Molnár and J. Sommer, John Wiley & Sons, Inc., Hoboken, New Jersey, 2nd edn, 2009.
- A. A. Danopoulos, J. R. Galsworthy, M. L. H. Green, S. Cafferkey, L. H. Doerrer and M. B. Hursthouse, *Chem. Commun.*, 1998, 2529.
- C. Bergquist, B. M. Bridgewater, C. J. Harlan, J. R. Norton, R. A. Friesner and G. Parkin, *J. Am. Chem. Soc.*, 2000, **122**, 10581.
- (a) R. Duchateau, R. A. van Santen and G. P. A. Yap, *Organometallics*, 2000, **19**, 809; (b) R. T. Stibrany and P. Brant, *Acta Crystallogr., Sect. C: Cryst. Struct. Commun.*, 2001, **57**, 644; (c) M. J. Drewitt, M. Niedermann and M. C. Baird, *Inorg. Chim. Acta*, 2002, **340**, 207; (d) A. Di Saverio, F. Focante, I. Camurati, L. Resconi, T. Beringhelli, G. D'Alfonso, D. Donghi, D. Maggioni, P. Mercandelli and A. Sironi, *Inorg. Chem.*, 2005, **44**, 5030; (e) F. Focante, I. Camurati, L. Resconi, S. Guidotti, T. Beringhelli, G. D'Alfonso, D. Donghi, D. Maggioni, P. Mercandelli and A. Sironi, *Inorg. Chem.*, 2006, **45**, 1683; (f) F. Focante, P. Mercandelli, A. Sironi and L. Resconi, *Coord. Chem. Rev.*, 2006, **250**, 170.
- (a) G. S. Hill, L. Manojlovic-Muir, K. W. Muir and R. J. Puddephatt, *Organometallics*, 1997, **16**, 525; (b) L. Doerrer and M. L. H. Green, *J. Chem. Soc., Dalton Trans.*, 1999, 4325; (c) D. Neculai, H. W. Roesky, A. M. Neculai, J. Magull, B. Walfort and D. Stalke, *Angew. Chem., Int. Ed.*, 2002, **41**, 4294; (d) G. Schatte, T. Chivers, H. M. Tuononen, R. Suontamo, R. Laitinen and J. Valkonen, *Inorg. Chem.*, 2005, **44**, 443; (e) J. Sánchez-Nieves, L. M. Frutos, P. Royo, O. Castaño and E. Herdtweck, *Organometallics*, 2005, **24**, 2004; (f) J. Sánchez-Nieves, L. M. Frutos, P. Royo, O. Castaño, E. Herdtweck and M. E. G. Mosquera, *Inorg. Chem.*, 2010, **49**, 10642.
- (a) M. A. Beckett, D. S. Brassington, S. J. Coles and M. B. Hursthouse, *Inorg. Chem. Commun.*, 2000, **3**, 530; (b) M. A. Beckett, D. S. Brassington, M. E. Light and M. B. Hursthouse, *J. Chem. Soc., Dalton Trans.*, 2001, 1768; (c) A. J. P. Cardenas, B. J. Culotta, T. H. Warren, S. Grimme, A. Stute, R. Fröhlich, G. Kehr and G. Erker, *Angew. Chem., Int. Ed.*, 2011, **50**, 7567.
- (a) J. Tian, S. Wang, Y. Feng, J. Li and S. Collins, *J. Mol. Catal. A: Chem.*, 1999, **144**, 137; (b) T. Beringhelli, G. D'Alfonso, D. Donghi, D. Maggioni, P. Mercandelli and A. Sironi, *Organometallics*, 2003, **22**, 1588; (c) A. Y. Timoshkin and G. Frenking, *Organometallics*, 2008, **27**, 371.
- (a) K. Diemert, U. Englert, W. Kuchen and F. Sandt, *Angew. Chem., Int. Ed.*, 1997, **36**, 241; (b) M. G. Walawalkar, R. Murugavel, H. W. Roesky and H.-G. Schmidt, *Organometallics*, 1997, **16**, 516; (c) M. G. Walawalkar, R. Murugavel, H. W. Roesky and H.-G. Schmidt, *Inorg. Chem.*, 1997, **36**, 4202; (d) J. Mortier, I. D. Gridnev and P. Guénot, *Organometallics*, 2000, **19**, 4266; (e) J. Tönnemann, R. Scopelliti, K. O. Zhurov, L. Menin, S. Dehnen and K. Severin, *Chem. – Eur. J.*, 2012, **18**, 9939–9945; (f) Q. Liu, N. D. Kontrella, A. S. Filatov and R. F. Jordan, *Organometallics*, 2015, **34**, 254.
- J. Beckmann, D. Dakternieks, A. E. K. Lim, K. F. Lim and K. Jurkschat, *THEOCHEM*, 2006, **761**, 177.
- I. Haiduc, *Organometallics*, 2004, **23**, 3.
- T. Steiner, *Angew. Chem., Int. Ed.*, 2002, **41**, 49.
- J. Bernstein, R. E. Davis, L. Shimoni and N.-L. Chang, *Angew. Chem., Int. Ed.*, 1995, **34**, 1555.
- K. F. Bowes, C. Glidewell and J. N. Low, *Acta Crystallogr., Sect. C: Cryst. Struct. Commun.*, 2002, **58**, o409.
- M. J. Frisch, *et al.*, *Gaussian09, Revision B.01*, Gaussian, Inc., Wallingford, CT, 2010. See ESI† for the computational details.
- (a) J. Guo, W.-K. Wong and W.-Y. Wong, *Polyhedron*, 2005, **24**, 927; (b) K. A. Lyssenko, G. V. Grintsev-Knyazev and M. Yu. Antipin, *Mendeleev Commun.*, 2002, **12**, 128.
- $\text{p}K_{\text{a}}(\text{gas})$ were calculated on the basis of the M052X/6-31+G** sums of the electronic and thermal Gibbs free energies; $\text{p}K_{\text{a}}(\text{MeCN})$ were estimated at the same level of theory using the SMD solvation model: A. V. Marenich, C. J. Cramer and D. G. Truhlar, *J. Phys. Chem. B*, 2009, **113**, 6378. See ESI† for the details of calculations.
- $\text{p}K_{\text{a}}(\text{exp})$ were obtained from the gas-phase acidity (GA) values: J. E. Bartmess, in *NIST Chemistry WebBook, NIST Standard Reference Database Number 69*, ed. P. J. Linstrom and W. G. Mallard, NIST, Gaithersburg, MD, 20899, <http://webbook.nist.gov>.
- A. Kütt, I. Leito, I. Kaljurand, L. Soovali, V. M. Vlasov, L. M. Yagupolskii and I. A. Koppel, *J. Org. Chem.*, 2006, **71**, 2829.
- J. Beckmann, D. Dakternieks, A. Duthie and C. Mitchell, *Organometallics*, 2003, **22**, 2161.
- U. Kolb, M. Beuter and M. Dräger, *Inorg. Chem.*, 1994, **33**, 4522.
- (a) M. Schmeisser, P. Sartori and B. Lippsmeier, *Chem. Ber.*, 1970, **103**, 868; (b) J. Beckmann, E. Lork and O. Mallow, *Main Group Met. Chem.*, 2012, **35**, 183.
- X. Wang and P. P. Power, *Angew. Chem., Int. Ed.*, 2011, **50**, 10965.

